Correspondence and
requests for materials
should be addressed to
F.W.H. (fwhuo@ntu.
edu.sg) or C.Y.Y.T.
(tangc@hku.hk)

Fabrication of Porous Matrix Membrane (PMM) Using Metal-Organic Framework as Green Template for Water Treatment

Jian-Yuan Lee[1,2], Chuyang Y. Tang[1,2,3] & Fengwei Huo[1,2,4]

[1]Nanyang Environment & Water Research Institute, Interdisciplinary Graduate School, Nanyang Technological University, Singapore, 639798, [2]Singapore Membrane Technology Centre, Nanyang Environment & Water Research Institute, Nanyang Technological University, Singapore, 637141, [3]Department of Civil Engineering, the University of Hong Kong, Pokfulam, Hong Kong, [4]School of Materials Science and Engineering, Nanyang Technological University, Singapore, 639798.

Pressure-driven membranes with high porosity can potentially be fabricated by removing template, such as low water stability metal-organic frameworks (MOFs) or other nanoparticles, in polymeric matrix. We report on the use of benign MOFs as green template to enhance porosity and interconnectivity of the water treatment membranes. Significantly enhanced separation performance was observed which might be attributed to the mass transfer coefficient of the substrate layer increased in ultrafiltration (UF) application.

With the increasing world population, the demand for clean drinking water also increases exponentially[1]. One of the most challenging global problems affecting many countries around the world is clean water shortage and thus growing concerns over the access to safe drinking water[2]. To meet this challenge, membrane-based water treatment processes have become one of the most energy efficient and most reliable technologies for supplying water[3,4]. Compared to conventional thermal distillation processes, membrane-based water treatment processes have relatively lower energy consumption, improved cost effectiveness, and ensuring a more sustainable production of drinking water in the future[2,5]. Hence, membrane-based water treatment processes have been employed in a wide range of applications such as oil/water separation[6–10] wastewater treatment[11–14], water purification[15–17], seawater desalination[18–21], food processing[22–24], and valuable product recovery[25–30].

In pressure-driven membrane processes, such as ultrafiltration (UF), nanofiltration (NF), and reverse osmosis (RO), an external pressure is applied on the solution at one side of the semi-permeable membrane, which serves as a driving force to separate water effectively from the pollutant in the feed solution[31,32]. In general, the permeate flux of water, J_v is directly related to the driving force, ΔP, times the water permeability coefficient, A. The water permeability coefficient is mainly determined by the membrane structure, such as porosity, pore diameter, and tortuosity. In theory, an ideal membrane is expected to have highly porous but very thin and low tortuosity structure. Therefore, higher porosity of membrane will result in higher water permeability coefficient and therefore the higher flux of the membrane processes. Previous studies showed that a variety of additives such as LiCl, polyvinylpyrrolidone (PVP), polyethylene glycol (PEG) were added into the polymer dope solution in order to promote the pore formation[33]. However, all these additives can easily dissolve in the polar organic solvent such as dimethylformamide (DMF) and N-methyl-2-pyrrolidone (NMP), and was removed during the non-solvent induced phase inversion (NIPS), which resulted in lower porosity. Alternatively, mixed matrix membrane (MMM) is an emerging strategy to enhance several intrinsic membrane properties of pressure-driven membranes. For example, water permeability, anti-fouling property, thermal and mechanical stability of pressure-driven membranes can be potentially enhanced by incorporating nanomaterials such as zeolite[34–40], silica nanoparticle[41–43], titanium oxide nanoparticle[44], and silver nanoparticle[45,46]. However, poor dispersion of the filler in the polymer matrix and incompatibility issue between the polymer and filler might result in poor selectivity of the MMMs[47,48]. Herein, we proposed the use of benign metal-organic frameworks (MOFs) as green template for the formation of macropores to enhance porosity and interconnectivity of the water treatment membranes.

Our basic idea is to construct a porous matrix membrane (PMM) using MOF particles as template, which initially cannot dissolve in the polar organic solvent but can be easily washed away by water. We believe that our strategy might potentially further improve the porosity of the membranes after removal of these particles (Figure 1). In addition, compared to conventional etching methods, such as the removal of silica nanoparticle by hydrofluoric acid or the removal of gold nanoparticle by potassium iodide, our strategy uses water as the
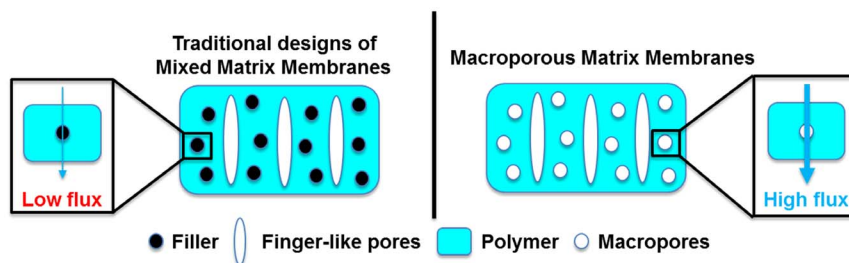
Figure 1 | Schematic representation of our strategy compared with traditional mixed matrix membranes.

etching solution, which is low cost, environmental-friendly and easily available. Herein, we report on the use of MOFs as green template to enhance porosity and interconnectivity of the water treatment membranes. MOFs were chosen as the templates because of some of MOFs have relatively low water stability compared to zeolite and silica gel but relatively high stability in organic solvents. Firstly, we studied the dispersion of MOF as filler by embedding less water soluble MOF (F300, iron benzene-1,3,5-tricarboxylate) into polyacrylonitrile (PAN) as a negative control. Secondly, we chose two types of hydrophilic MOF (A100, aluminium terephthalate and C300, copper benzene-1,3,5-tricarboxylate), which is relatively lower water stability than the F300 as the green template. Lastly, the morphology and structure of MOF-based MMMs and PMMs were systematically characterized by field emission scanning electron microscopy (FESEM) and energy-dispersive X-ray spectroscopy (EDX). We speculated that the performance enhancement of pressure driven membrane process is due to the mass transfer coefficient of the PMM increased in ultrafiltration (UF) application.

Results

Firstly, the morphology information and water stability of MOF (A100, C300, and F300) in pure water were shown in Figure 2. A100 is a grey powder while F300 is an orange powder as observed by naked eyes. Both A100 and F300 showed as irregular shaped fine particle under the observation of FESEM. On the other hand, C300 is a blue powder and stone-like particle under the observation of FESEM. Both A100 and C300 showed relatively low water stability and can be completely dissolved in pure water compared to F300, which showed relatively high water stability and can only partially dissolved in aqueous solution.

The preparation of PMMs is outlined in Figure 3. MOFs were firstly dispersed in the DMF by ultrasonicating the solution for
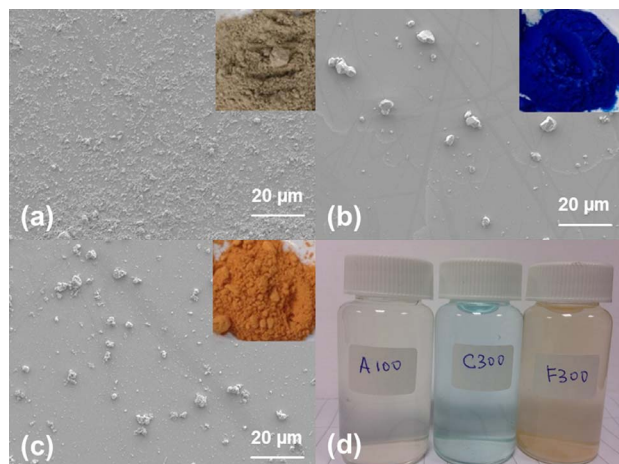
1 hour. Polymer and LiCl were then added into the DMF solution followed by stirring for at least 24 h at 60°C until a homogeneous solution was obtained. A casting knife was used to cast the polymer solution onto a clean glass plate. The polymer film was then immersed into the tap water bath at room temperature followed by soaking in continuous flow water bath to completely remove the MOF as well as the excess solvent inside the membrane. The advantages of our strategy including: 1) MOFs were used as green template, which can be easily removed by water without using toxic chemical, strong acid or base; 2) the fabrication process is under mild condition: neutral pH, at room temperature and under atmospheric pressure; 3) the processes is environmental-friendly, which
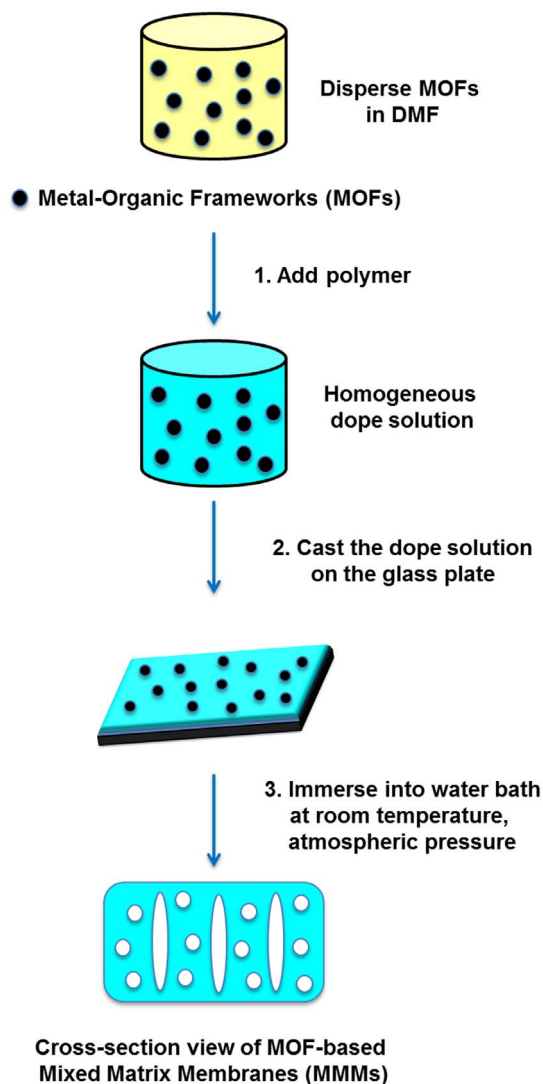

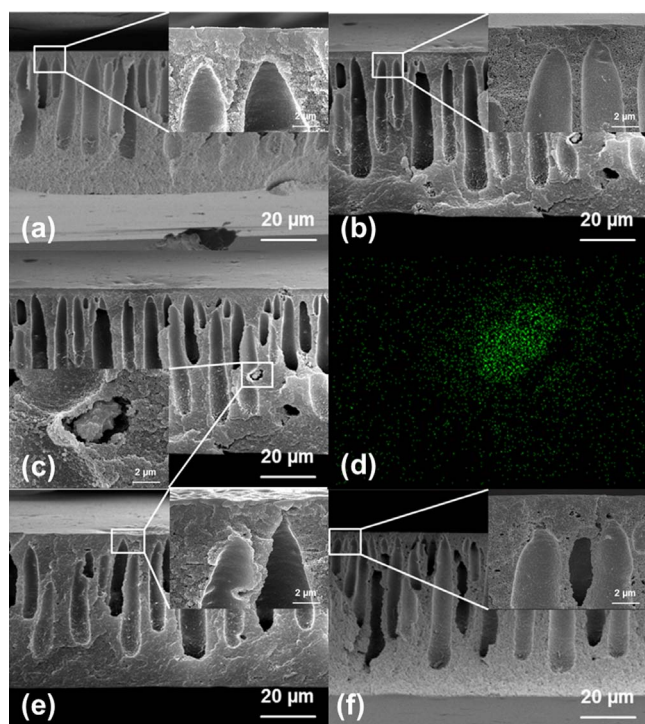**Figure 3 | Schematic diagram of the preparation of PMMs.**

Figure 2 | The FESEM characterization of MOF. (a) A100, (b) C300, (c) F300. The inset is the camera image of MOF. (d) The water stability of MOF in pure water.

2

Figure 4 | FESEM micrographs of cross-section of (a) control, (b) PMM$_{F300}$, (c) PMM$_{F300}$, inset: enlarged image of F300, which cannot be completely remove under neutral condition, (d) EDX image of the enlarged image, (e) PMM$_{A100}$, (f) PMM$_{C300}$.

minimizes the use of chemicals and reduces the impact on the environment; 4) our strategy is compatible with the current membrane manufacturing processes without extra steps or modification; 5) MOFs is commercial viable, low cost and could be easily scale-up.

Figure 4 showed the FESEM and EDX images of cross sections of PMMs and MMMs. The separation performance and the porosity of the PMMs compared with the control and MMM were shown in Figure 5. The cross-section images of a control, which represent the commercial UF membrane and a negative control (F300), which represent MOF-based MMM were shown in Figure 4 (a) and (b). The presence of MOF (F300) can still be observed using FESEM and further confirmed by EDX analysis (Figure 4 (c) and (d)). These results proved that the MOF were successfully incorporated into the polymer matrix and good dispersion was achieved after

sonication. Correspondingly, the marginal increased in water permeability and porosity were observed in Figure 5 (a) and (b). This might be explained by the partial dissolution of F300 under neutral pH condition[49,50].

Discussion

More importantly, the successful removal of MOF particle was confirmed by FESEM as shown in Figure 4 (e) and (f). Significant amount of macropores were created in the polymer matrix. As a result, a highly porous PMM$_{C300}$ with porosity of $83\pm2\%$ based on gravimetric measurement was obtained (Figure 5 (b)). Generally, a membrane substrate with high porosity is generally more favored due to increase the mass transfer of water in pressure-driven membrane processes. Indeed, the highly porous matrix ultrafiltration membranes (PMM$_{A100}$ and PMM$_{C300}$) generally showed higher water permeability without compromising the rejection of dextran. The highest water permeability of 260.5 L/m^2 h bar was achieved for PMM$_{C300}$, which probably due to the combination of enhanced porosity and interconnectivity of the ultrafiltration membranes. It is important to note that the dextran rejection did not significantly change between control and highly porous PMM after removal of MOF in the substrate layer, which means the membrane selectivity remain unchanged. Our overall results clearly show that the removal of MOFs in the polymer matrix substantially enhanced the porosity and is a promising strategy for better separation performance of pressure-driven membranes.

In order to determine the residual amount of MOFs inside the PMM membrane, the PMM samples were digested with a mixture of concentrated nitric acid and concentrated hydrochloric acid in the ratio of 3 : 1 for 6 hours followed by topping up the concentrated acid solution to 10 mL with water. Precipitates were observed at the bottom of the bottles prior to inductively coupled plasma (ICP) analysis, which can determine metal ions in aqueous solutions down to part per millions (ppm) or even part per billions (ppb) level. Indeed, the PMM$_{F300}$ has the highest residual percentage of iron (24.0 ± 6.9 wt%). In comparison, PMM$_{A100}$ has significantly lower residual percentage of aluminium (8.4 ± 0.6 wt%) and PMM$_{C300}$ has the lowest residual percentage of copper (3.8 ± 0.4 wt%) among the three PMM samples. It is noteworthy that the order of membrane water permeability (F300<A100<C300) coincides with the (reverse) order of water stability and residual percentage of MOF (F300>A100>C300). Thus, one reasonable explanation for the highest water permeability of PMM$_{C300}$ is the higher water solubility of C300. The enhanced pore connectivity in addition to improved porosity is likely responsible to the marked increased in membrane
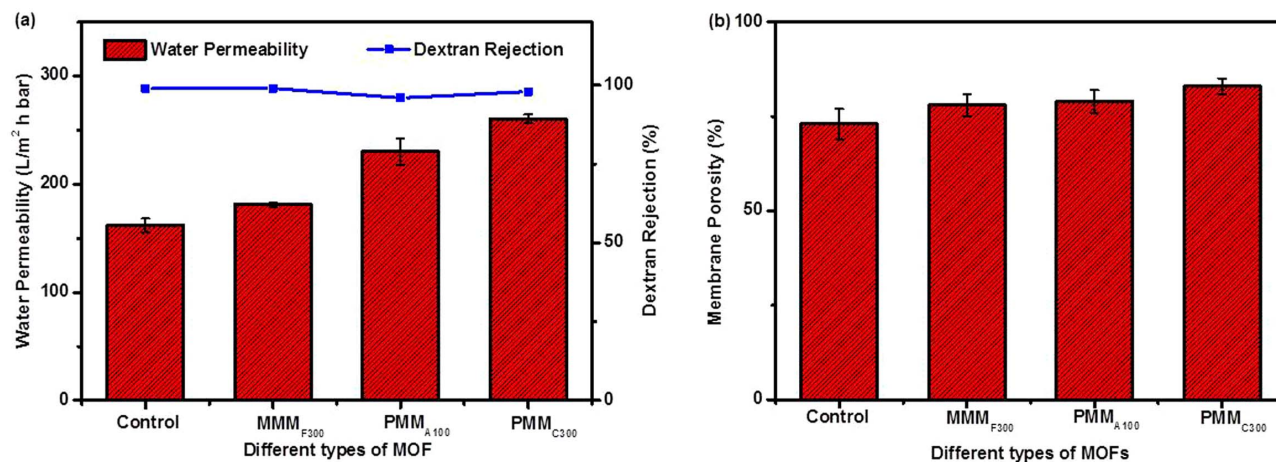

Figure 5 | Effect of different types of MOF on the performance of pressure-driven ultrafiltration membranes (a) the pure water permeability and dextran rejection of the ultrafiltration membranes; (Testing conditions: DI water or dextran solution as the feed solution; applied pressure: 5 bars) and (b) membrane porosity.

water permeability. However, the authors admitted that other important parameters, such as the loading, shape, and size of MOF particles, water stability of MOFs, and other types of water soluble MOFs or other kinds of nanomaterials should be optimized to further enhance of the performance of PMM membranes.

In summary, MOF-based MMMs and PMM were systematically synthesized and characterized in this study. PMMs can significantly enhance water permeability in pressure driven membrane processes probably due to the removal of MOF particles in the polymer matrix, which enhanced membrane porosity and interconnectivity of the membrane. More importantly, the current study demonstrates MOFs as green template might have good potential for not only pressure-driven membranes processes but also for carbonaceous nannofiber membranes for selective filtration and separation of nanoparticle[16,27], or osmotically-driven membrane process, such as forward osmosis (FO) and pressure-retarded osmosis (PRO)[51,52].

Methods

Materials. Polyacrylonitrile (PAN, weight averaged molecular weight Mw ~150,000, Sigma–Aldrich, Lot# MKBN2648V), N,N-dimethylformamide (DMF, ≥99.8%, Merck), and lithium chloride (LiCl, anhydrous, Merck) were used as the polymer, the solvent, and the pore former, respectively, for casting membrane substrates. Basolite A100 (Aluminium terephthalate or MIL 53, product # 688738, produced by BASF, Sigma-Aldrich, Lot#STBC4615V), Basolite C300 (Copper benzene-1,3,5-tricarboxylate or HKUST-1, product # 688614, produced by BASF, Sigma-Aldrich, Lot#STBC4614V), Basolite F300 (Iron benzene-1,3,5-tricarboxylate or Fe-BTC, product # 690872, produced by BASF, Sigma-Aldrich, Lot#S61151V) were used for membrane preparation. All chemicals were used as received.

Typical procedure for fabrication of porous matrix membrane (PMM). To achieve good dispersion of the particles, 1.0 wt.% of MOF particles were added into DMF followed by ultrasonicating the solution for 1 h. PAN (18 wt.%) and LiCl (2 wt.%) were then added into the DMF solution followed by stirring for at least 24 h at 60°C until a homogeneous solution was obtained. The polymer solution was then cooled down to room temperature overnight without stirring to completely remove any gas bubbles. A casting knife (Elcometer Pte. Ltd., Asia) was used to spread the polymer solution onto a clean glass plate at a gate height of 150 μm. The plate was then immersed into tape water at room temperature for 10 min till the PAN substrate was separated from the glass plate. The resulting membrane substrate was soaked in tap water bath followed by deionized (DI) water rinsing and the resulting membrane was designated as (Control, MMM$_{F300}$, PMM$_{A100}$, and PMM$_{C300}$).

Membrane characterization. The surface and cross section morphological structures of the prepared PAN membranes were characterized by field emission scanning electron microscope (FESEM, JSM-7600F, USA). A freeze-dryer was used to dry all the membranes samples at room temperature for at least 12 h followed by coated with a uniform platinum layer before observation. Element mapping was detected with the FESEM microscope equipped with energy-dispersive X-ray spectroscopy (EDX, Oxford Instrument, UK). The methods for determining intrinsic separation properties such as pure water permeability and dextran rejection can be found elsewhere[53,54]. Briefly, all the membranes were tested in a pressurised cross flow filtration setup using an applied pressure of 5 bars and the feed water temperature remained at 20 °C by a circulating cooling system. The effective membrane area was 42 cm². A relatively high cross flow velocity of 20 cm/s and diamond-shaped feed spacers were used to reduce the concentration polarization of feed solutes. By measuring the amount of permeate, the water permeability coefficient A of membranes was determined. The dextran rejection was determined by gel permeation chromatography (GPC, Varian Company, USA) with the difference between the feed water and permeates water. The reported values of A and R are the average value of at least three replicates.

Gravimetric measurement. The membrane porosity, ε, was defined as the volume of the pores divided by the total volume of the membrane. It can be determined by gravimetric method, measuring the weight of water contained in the membrane pores. By measuring the dry mass (m$_{dry}$) and wet mass (m$_{wet}$) of membrane samples, the membrane porosity (ε) can be calculated according to following equation (1):

$$\varepsilon = \frac{(m_{wet}-m_{dry})/\rho_w}{(m_{wet}-m_{dry})/\rho_w + m_{dry}/\rho_m} \times 100\% \quad (1)$$

where ρ_w and ρ_m are the density of water (1.0 g/cm³) and the density of PAN (1.18 g/cm³). It was assumed that all the pores in the membrane and silica gel were completely filled with water.

1. Elimelech, M. & Phillip, W. A. The Future of Seawater Desalination: Energy, Technology, and the Environment. *Science* **333**, 712–717 (2011).
2. Shannon, M. A. *et al.* Science and technology for water purification in the coming decades. *Nature* **452**, 301–310 (2008).
3. Service, R. F. Desalination Freshens Up. *Science* **313**, 1088–1090 (2006).
4. Logan, B. E. & Elimelech, M. Membrane-based processes for sustainable power generation using water. *Nature* **488**, 313–319 (2012).
5. Van der Bruggen, B. & Vandecasteele, C. Distillation vs. membrane filtration: overview of process evolutions in seawater desalination. *Desalination* **143**, 207–218 (2002).
6. Shi, Z. *et al.* Ultrafast Separation of Emulsified Oil/Water Mixtures by Ultrathin Free-Standing Single-Walled Carbon Nanotube Network Films. *Adv. Mater.* **25**, 2422–2427 (2013).
7. Zhang, F. *et al.* Nanowire-haired inorganic membranes with superhydrophilicity and underwater ultralow adhesive superoleophobicity for high-efficiency oil/water separation. *Adv. Mater.* **25**, 4192–4198 (2013).
8. Zhang, W., Shi, Z., Zhang, F., Liu, X., Jin, J. & Jiang, L. Superhydrophobic and Superoleophilic PVDF Membranes for Effective Separation of Water-in-Oil Emulsions with High Flux. *Adv. Mater.* **25**, 2071–2076 (2013).
9. Maphutha, S., Moothi, K., Meyyappan, M. & Iyuke, S. E. A carbon nanotube-infused polysulfone membrane with polyvinyl alcohol layer for treating oil-containing waste water. *Sci. Rep.* **3**, 1509; DOI:10.1038/srep01509 (2013).
10. Chen, P. & Xu, Z. Mineral-Coated Polymer Membranes with Superhydrophilicity and Underwater Superoleophobicity for Effective Oil/Water Separation. *Sci. Rep.* **3**, 2776; DOI:10.1038/srep02776 (2013).
11. Zhang, X., Zhang, T., Ng, J. & Sun, D. D. High-Performance Multifunctional TiO2 Nanowire Ultrafiltration Membrane with a Hierarchical Layer Structure for Water Treatment. *Adv. Funct. Mater.* **19**, 3731–3736 (2009).
12. Greenlee, L. F., Lawler, D. F., Freeman, B. D., Marrot, B. & Moulin, P. Reverse osmosis desalination: Water sources, technology, and today's challenges. *Water Res.* **43**, 2317–2348 (2009).
13. Pérez-González, A., Urtiaga, A. M., Ibáñez, R. & Ortiz, I. State of the art and review on the treatment technologies of water reverse osmosis concentrates. *Water Res.* **46**, 267–283 (2012).
14. Gao, Y., de Jubera A. M. S., Mariñas, B. J. & Moore, J. S. Nanofiltration Membranes with Modified Active Layer Using Aromatic Polyamide Dendrimers. *Adv. Funct. Mater.* **23**, 598–607 (2013).
15. Sekulić, J., ten Elshof, J. E. A. & Blank, D. H. A Microporous Titania Membrane for Nanofiltration and Pervaporation. *Adv. Mater.* **16**, 1546–1550 (2004).
16. Liang, H.-W. *et al.* Robust and Highly Efficient Free-Standing Carbonaceous Nanofiber Membranes for Water Purification. *Adv. Funct. Mater.* **21**, 3851–3858 (2011).
17. Han, Y., Xu, Z. & Gao, C. Ultrathin Graphene Nanofiltration Membrane for Water Purification. *Adv. Funct. Mater.* **23**, 3693–3700 (2013).
18. Kessler, J. O. & Moody, C. D. Drinking water from sea water by forward osmosis. *Desalination* **18**, 297–306 (1976).
19. Lee, K. P., Arnot, T. C. & Mattia, D. A review of reverse osmosis membrane materials for desalination—Development to date and future potential. *J. Membr. Sci.* **370**, 1–22 (2011).
20. Misdan, N., Lau, W. J. & Ismail, A. F. Seawater Reverse Osmosis (SWRO) desalination by thin-film composite membrane—Current development, challenges and future prospects. *Desalination* **287**, 228–237 (2012).
21. Gu, J. E. *et al.* Molecular Layer-by-Layer Assembled Thin-Film Composite Membranes for Water Desalination. *Adv. Mater.* **25**, 4778–4782 (2013).
22. Álvarez, S., Riera, F. A., Álvarez, R. & Coca, J. Concentration of Apple Juice by Reverse Osmosis at Laboratory and Pilot-Plant Scales. *Ind. Eng. Chem. Res.* **41**, 6156–6164 (2002).
23. Matta, V. M., Moretti, R. H. & Cabral, L. M. C. Microfiltration and reverse osmosis for clarification and concentration of acerola juice. *J. Food Eng.* **61**, 477–482 (2004).
24. Souza, A. L. R., Pagani, M. M., Dornier, M., Gomes, F. S., Tonon, R. V. & Cabral, L. M. C. Concentration of camu–camu juice by the coupling of reverse osmosis and osmotic evaporation processes. *J. Food Eng.* **119**, 7–12 (2013).
25. Pink, C. J., Wong, H.-t., Ferreira, F. C. & Livingston, A. G. Organic Solvent Nanofiltration and Adsorbents; A Hybrid Approach to Achieve Ultra Low Palladium Contamination of Post Coupling Reaction Products. *Org. Process Res. Dev.* **12**, 589–595 (2008).
26. Nair, D. *et al.* Extending Ru-BINAP Catalyst Life and Separating Products from Catalyst Using Membrane Recycling. *Org. Process Res. Dev.* **13**, 863–869 (2009).
27. Liang, H.-W. *et al.* Carbonaceous Nanofiber Membranes for Selective Filtration and Separation of Nanoparticles. *Adv. Mater.* **22**, 4691–4695 (2010).
28. Sereewatthanawut, I. *et al.* Demonstration of Molecular Purification in Polar Aprotic Solvents by Organic Solvent Nanofiltration. *Org. Process Res. Dev.* **14**, 600–611 (2010).
29. So, S., Peeva, L. G., Tate, E. W., Leatherbarrow, R. J. & Livingston, A. G. Organic Solvent Nanofiltration: A New Paradigm in Peptide Synthesis. *Org. Process Res. Dev.* **14**, 1313–1325 (2010).
30. Liu, X.-L. *et al.* An Organophilic Pervaporation Membrane Derived from Metal–Organic Framework Nanoparticles for Efficient Recovery of Bio-Alcohols. *Angew. Chem. Int. Ed.* **50**, 10636–10639 (2011).
31. Petersen, R. J. Composite reverse osmosis and nanofiltration membranes. *J. Membr. Sci.* **83**, 81–150 (1993).

32. Van Der Bruggen, B., Vandecasteele, C., Van Gestel, T., Doyen, W. & Leysen, R. A review of pressure-driven membrane processes in wastewater treatment and drinking water production. *Environ. Prog.* **22**, 46–56 (2003).

33. Guillen, G. R., Pan, Y., Li, M. & Hoek, E. M. V. Preparation and Characterization of Membranes Formed by Nonsolvent Induced Phase Separation: A Review. *Ind. Eng. Chem. Res.* **50**, 3798–3817 (2011).

34. Jeong, B. H. *et al.* Interfacial polymerization of thin film nanocomposites: A new concept for reverse osmosis membranes. *J. Membr. Sci.* **294**, 1–7 (2007).

35. Lind, M. L. *et al.* Influence of Zeolite Crystal Size on Zeolite-Polyamide Thin Film Nanocomposite Membranes. *Langmuir* **25**, 10139–10145 (2009).

36. Bae, T.-H. *et al.* Facile High-Yield Solvothermal Deposition of Inorganic Nanostructures on Zeolite Crystals for Mixed Matrix Membrane Fabrication. *J. Am. Chem. Soc.* **131**, 14662–14663 (2009).

37. Fathizadeh, M., Aroujalian, A. & Raisi, A. Effect of added NaX nano-zeolite into polyamide as a top thin layer of membrane on water flux and salt rejection in a reverse osmosis process. *J. Membr. Sci.* **375**, 88–95 (2011).

38. Ma, N., Wei, J., Liao, R. & Tang, C. Y. Zeolite-polyamide thin film nanocomposite membranes: Towards enhanced performance for forward osmosis. *J. Membr. Sci.* **405–406**, 149–157 (2012).

39. Ma, N. *et al.* Nanocomposite substrates for controlling internal concentration polarization in forward osmosis membranes. *J. Membr. Sci.* **441**, 54–62 (2013).

40. Kiesow, I., Marczewski, D., Reinhardt, L., Mühlmann, M., Possiwan, M. & Goedel, W. A. Bicontinuous Zeolite Polymer Composite Membranes Prepared via Float Casting. *J. Am. Chem. Soc.* **135**, 4380–4388 (2013).

41. Jadav, G. L. & Singh, P. S. Synthesis of novel silica-polyamide nanocomposite membrane with enhanced properties. *J. Membr. Sci.* **328**, 257–267 (2009).

42. Huang, J. *et al.* Fabrication of polyethersulfone-mesoporous silica nanocomposite ultrafiltration membranes with antifouling properties. *J. Membr. Sci.* **423**, 362–370 (2012).

43. Wu, H. Q., Tang, B. B. & Wu, P. Y. Optimizing polyamide thin film composite membrane covalently bonded with modified mesoporous silica nanoparticles. *J. Membr. Sci.* **428**, 341–348 (2013).

44. Lee, H. S. *et al.* Polyamide thin-film nanofiltration membranes containing TiO2 nanoparticles. *Desalination* **219**, 48–56 (2008).

45. Kim, E. S., Hwang, G., El-Din, M. G. & Liu, Y. Development of nanosilver and multi-walled carbon nanotubes thin-film nanocomposite membrane for enhanced water treatment. *J. Membr. Sci.* **394**, 37–48 (2012).

46. Liu, X. *et al.* Synthesis and characterization of novel antibacterial silver nanocomposite nanofiltration and forward osmosis membranes based on layer-by-layer assembly. *Water Res.* **47**, 3081–3092 (2013).

47. Shi, G. M., Yang, T. & Chung, T. S. Polybenzimidazole (PBI)/zeolitic imidazolate frameworks (ZIF-8) mixed matrix membranes for pervaporation dehydration of alcohols. *J. Membr. Sci.* **415–416**, 577–586 (2012).

48. Zornoza, B., Tellez, C., Coronas, J., Gascon, J. & Kapteijn, F. Metal organic framework based mixed matrix membranes: An increasingly important field of research with a large application potential. *Microporous Mesoporous Mater.* **166**, 67–78 (2013).

49. Henninger, S. K., Habib, H. A. & Janiak, C. MOFs as Adsorbents for Low Temperature Heating and Cooling Applications. *J. Am. Chem. Soc.* **131**, 2776–2777 (2009).

50. Jeremias, F., Khutia, A., Henninger, S. K. & Janiak, C. MIL-100(Al, Fe) as water adsorbents for heat transformation purposes-a promising application. *J. Mater. Chem.* **22**, 10148–10151 (2012).

51. Song, X., Liu, Z. & Sun, D. D. Nano Gives the Answer: Breaking the Bottleneck of Internal Concentration Polarization with a Nanofiber Composite Forward Osmosis Membrane for a High Water Production Rate. *Adv. Mater.* **23**, 3256–3260 (2011).

52. Song, X., Liu, Z. & Sun, D. D. Energy recovery from concentrated seawater brine by thin-film nanofiber composite pressure retarded osmosis membranes with high power density. *Energy Environ. Sci.* **6**, 1199–1210 (2013).

53. Tang, C. Y. Y., She, Q. H., Lay, W. C. L., Wang, R. & Fane, A. G. Coupled effects of internal concentration polarization and fouling on flux behavior of forward osmosis membranes during humic acid filtration. *J. Membr. Sci.* **354**, 123–133 (2010).

54. Wei, J., Qiu, C. Q., Tang, C. Y. Y., Wang, R. & Fane, A. G. Synthesis and characterization of flat-sheet thin film composite forward osmosis membranes. *J. Membr. Sci.* **372**, 292–302 (2011).

Author contributions

J.-Y. L. conceived the idea, designed and carried out the experiments, analyzed the data and co-drafted the manuscript. F.H. and C.Y.T. supervised the project, helped design the experiments and co-drafted the manuscript. All the authors contributed to the interpretation of the results and writing the manuscript.

Additional information